Intracellular pH gradients in migrating cells

Martin, Christine; Pedersen, Stine Helene Falsig; Schwab, Albrecht; Stock, Christian

Published in:
American Journal of Physiology: Cell Physiology

DOI:
10.1152/ajpcell.00280.2010

Publication date:
2011

Document Version
Publisher's PDF, also known as Version of record

Intracellular pH gradients in migrating cells

Christine Martin, Stine F. Pedersen, Albrecht Schwab and Christian Stock

Am J Physiol Cell Physiol 300:C490-C495, 2011. First published 9 December 2010;
doi: 10.1152/ajpcell.00280.2010

American Journal of Physiology - Cell Physiology is dedicated to innovative approaches to the study of cell and molecular physiology. It is published 12 times a year (monthly) by the American Physiological Society, 9650 Rockville Pike, Bethesda MD 20814-3991. ISSN: 0363-6143, ESSN: 1522-1563. Visit our website at http://www.the-aps.org/.

Am J Physiol Cell Physiol 300: C490–C495, 2011.
First published December 9, 2010; doi:10.1152/ajpcell.00280.2010.

Intracellular pH gradients in migrating cells

Christine Martin,[1] Stine F. Pedersen,[2] Albrecht Schwab,[1] and Christian Stock[1]

[1]*Institute of Physiology II, University of Muenster, Muenster, Germany; and* [2]*Section for Cell and Developmental Biology, Department of Biology, University of Copenhagen, Copenhagen, Denmark*

Submitted 20 July 2010; accepted in final form 6 December 2010

Martin C, Pedersen SF, Schwab A, Stock C. Intracellular pH gradients in migrating cells. *Am J Physiol Cell Physiol* 300: C490–C495, 2011. First published December 9, 2010; doi:10.1152/ajpcell.00280.2010.— Cell polarization along the axis of movement is required for migration. The localization of proteins and regulators of the migratory machinery to either the cell front or its rear results in a spatial asymmetry enabling cells to simultaneously coordinate cell protrusion and retraction. Protons might function as such unevenly distributed regulators as they modulate the interaction of focal adhesion proteins and components of the cytoskeleton in vitro. However, an intracellular pH (pH_i) gradient reflecting a spatial asymmetry of protons has not been shown so far. One major regulator of pH_i, the Na^+/H^+ exchanger NHE1, is essential for cell migration and accumulates at the cell front. Here, we test the hypothesis that the uneven distribution of NHE1 activity creates a pH_i gradient in migrating cells. Using the pH-sensitive fluorescent dye BCECF, pH_i was measured in five cell lines (MV3, B16V, NIH3T3, MDCK-F1, EA.hy926) along the axis of movement. Differences in pH_i between the front and the rear end (ΔpH_i front-rear) were present in all cell lines, and inhibition of NHE1 either with HOE642 or by absence of extracellular Na^+ caused the pH_i gradient to flatten or disappear. In conclusion, pH_i gradients established by NHE1 activity exist along the axis of movement.

cell migration; cell polarization; melanoma; NHE1; protons

CELL MIGRATION IS A MULTISTEP process and requires the precise coordination of adhesion to the matrix and cell protrusion at the leading edge as opposed to detachment from the matrix and cell retraction at the rear end. Hence, one essential characteristic of migrating cells is their polarization along the direction of movement (27). This morphological and functional polarization is based on an uneven distribution of adhesion proteins (23), ion channels and transporters (30), and signaling molecules (27). The importance of spatial asymmetry in migrating cells has been shown for small GTPases (Rho, Rac, and Cdc42) (27), lipid signaling (27), and cytosolic Ca^{2+} (31). Recent studies indicate that also the intracellular pH (pH_i) may serve locally as a regulator of cell polarization and migration (38) because it modulates cytoskeletal dynamics directly by affecting the actin-binding proteins talin (35) and cofilin (9) and indirectly by enhancing Cdc42 signaling (10, 17).

One important regulator of pH_i is the Na^+/H^+ exchanger NHE1, which accumulates at the leading edge (16) and expels protons from the cytosol (24). As part of focal adhesion contacts (22), NHE1 activity is of fundamental importance for cell migration, e.g., in fibroblasts (4, 29) and tumor cells (39). It has been hypothesized for quite a long time that the uneven distribution of NHE1 along the cell membrane contributes to differences in the local pH_i with the lamellipodia being more alkaline (4, 11). However, so far the postulated pH_i gradient has not been demonstrated experimentally in migrating cells.

Address for reprint requests and other correspondence: C. Stock, Institute of Physiology II, Robert-Koch-Str. 27b, D-48149 Münster, Germany (e-mail: cmstock@uni-muenster.de).

MATERIALS AND METHODS

Cells and Cell Culture

All cells were grown at 37°C in a humidified atmosphere of 5% CO_2-95% air. A human cell line [MV3 (43)] and a murine [B16V (8)] melanoma cell line were grown in bicarbonate-buffered RPMI 1640 (Sigma, Taufkirchen, Germany), transformed Madin-Darby canine kidney epithelial (MDCK-F) cells (21) in Earle's MEM (PAA), and the EA.hy926 human endothelial cell line (7) and NIH3T3 mouse fibroblasts (14) in DMEM 41965 (GIBCO). All media were supplemented with 10% fetal bovine serum.

The five cell lines were chosen since, although of completely different origin, all of them share the ability to polarize and to feature intrinsic migratory activity without being in need of additional stimuli or specific directional cues. Under subconfluent conditions, the typical migration speeds in single, unstimulated, randomly migrating cells come to (μm/min) ~0.7 in MV3 (36), ~0.4 in B16V [$n = 25$ cells from $N = 4$ experiments, unpublished observations; in B16-F10 up to 1 μm/min (20)], 0.8 in MDCK-F (5, 33), ~0.49 in EA.hy926 cells [$n = 16$ cells from $N = 4$ experiments; unpublished observations; (44)] and to ~0.7 μm/min in NIH3T3 fibroblasts (32).

Experimental Solutions

Measurements of pH_i were performed using HEPES-buffered Ringer solutions of pH 7.0 containing (in mmol/l) 122.5 NaCl, 5.4 KCl, 0.8 $MgCl_2$, 1.2 $CaCl_2$, 1.0 $NaH_2PO_4.2H_2O$, 5.0 glucose, and 10.0 HEPES. Ringer pH was adjusted by adding 1 M NaOH. For inhibition of NHE1, either HOE642 (Cariporide; 10 μmol/l) was added or the cells were superfused with a Na^+-free Ringer solution containing *N*-methyl-D-glucamine (NMDG) instead of Na^+. To check the contribution of bicarbonate (HCO_3^-) to the local, cytosolic pH, one set of experiments on MV3 cells was performed in HCO_3^--buffered Ringer solution of pH 7.0 containing (in mmol/l) 106.0 NaCl, 5.4 KCl, 0.8 $MgCl_2$, 1.2 $CaCl_2$, 0.8 $Na_2HPO_4 \times 2H_2O$, 0.2 $NaH_2PO_4 \times H_2O$, 24.0 $NaHCO_3$, and 5.5 glucose. pH was kept at 7.0 by continuous CO_2 gassing during the measurements [11.7% CO_2; P_{CO_2} in the experimental solution was 89 mmHg as determined by a blood gas analyzer (model ABL5, Radiometer, Brønshøj, Denmark)].

The pH of 7.0 was chosen because both the human (MV3) and the murine (B16) melanoma cells show their maximum migratory activity (36, 42) at this extracellular pH. Moreover, B16 cells are most invasive at pH 7.0 (42). And in tumors, the extracellular pH is generally more acidic than 7.4. For these reasons it is quite relevant to assess the motility at a lower pH.

Immunofluorescence of NHE1

Murine melanoma cells. B16V cells seeded on coverslips coated with a basement membrane-like matrix (in mg/ml: 0.4 collagen type IV, 0.003 laminin, 0.03 fibronectin in HEPES-buffered RPMI, pH 7.4) were treated with cold 0.2% Triton X-100 in phosphate-buffered saline (PBS) for 10 min before fixation. They were then fixed in 3.5% paraformaldehyde in PBS for 45 min at 4°C. Nonspecific binding sites were blocked with 2% BSA (wt/vol) and 0.2% (wt/vol) gelatine in

PBS. After the cells were stained with the primary antibody (hNHE1-mAb, BD Biosciences Pharmingen) for 1 h and a Cy3-conjugated secondary antibody for 45 min, the slide preparations were fixed once again, washed in PBS, and covered with Vectashield (Vector Laboratories, Burlingame, CA). Images were taken using an inverted microscope (Axiovert200, Carl Zeiss, Göttingen, Germany), a digital camera (model 9.0, RT-SE-Spot, Visitron Systems), and MetaVue software.

Murine fibroblasts. Immunofluorescence labeling of NHE1 in NIH3T3 cells was carried out essentially as previously described (26). Cells were fixed in 2% paraformaldehyde (15 min room temperature, 30 min on ice), washed in Tris-buffered saline (TBS), permeabilized for 10 min in 0.2% Triton X-100 in TBS, blocked for 30 min in 5% BSA in TBST (TBS + 0.1% Triton), incubated with rabbit polyclonal NHE1 antibody (a kind gift from Mark Musch, University of Chicago) 1:100 in TBST + 1% BSA (TBST-BSA) overnight at 4°C, washed in TBST-BSA, and incubated with AlexaFluor488-conjugated anti-rabbit secondary antibody (Invitrogen, 1:400 in TBST-BSA, 1 h), followed by further washes in TBST-BSA and mounting in *N*-propylgalleate mounting medium (2% wt/vol in PBS-glycerine). Cells were visualized using ×100/1.4 numerical aperture plan-apochromat objectives and the 488 nm Ar/Kr and 365 UV laser lines of a Leica DM-IRB/E microscope with a Leica TSC-NT confocal laser-scanning unit (Leica, Heidelberg, Germany). Optical slice thickness was 1 μm and pinhole size was 1 airy disc. Images were collected and frame-averaged using Leica software and processed (overlays and brightness/contrast adjustment only) using Adobe Photoshop.

Essentially, no labeling was detectable in the absence of primary antibody (not shown).

Measuring pH_i

pH_i was measured using video imaging techniques and the fluorescent pH indicator BCECF (Molecular Probes, Eugene, OR). MV3, MDCK-F, and NIH3T3 cells were plated onto coverslips coated with collagen type I (Biochrom, Berlin, Germany). B16V cells were plated onto coverslips coated with a basement membrane-like matrix (see above). Before polymerization, pH of this mixture was adjusted to 7.4 by adding 1 M NaOH. Cells were allowed to adapt for 3 h and were then incubated in the respective, HEPES- or HCO_3^--buffered, control solution containing 5 μg/ml BCECF-AM for 5 min. The coverslips were placed on the stage of an inverted microscope (Axiovert 200; Carl Zeiss) and continuously superfused with prewarmed (37°C) HEPES- or HCO_3^--buffered Ringer solution. Before ratiometric pH_i-measurement, the direction of migration, i.e., cell polarity, was checked by observing morphological changes in the moving cells, while during the actual pH_i-measurement the migratory activity was not further assessed. The excitation wavelengths were 440 nm and 490 nm, and the emitted fluorescence was monitored at 500 nm using a Photometrics camera (CoolSnap*fx*, Visitron Systems, Puchheim, Germany). The different wavelengths were generated by a high-speed polychromator system (Visichrome, Visitron Systems). Polychromator and data acquisition were controlled by Metaflour software (Visitron Systems). Fluorescence intensities were measured at 37°C in 35-s intervals and corrected for background fluorescence by subtracting intensities obtained from adjacent, extracellular regions. Exposure times were 100 and 250 ms for the 490- and the 440-nm image, respectively, and the camera gain used was 2. Flat field correction was not needed because the illumination across the visual field was uniform. At the end of each experiment, the pH measurements were calibrated by successively superfusing the cells with modified, high-K^+ Ringer solutions of pH 7.5, 7.0, and 6.5 containing (in mmol/l) 125 KCl, 1 $MgCl_2$, 1 $CaCl_2$, 20 HEPES, and 10 μmol/l nigericin (Sigma) (6).

To quantify pH_i along the direction of movement, the image of each cell was divided into three segments that represented the functionally different regions of a migrating cell: the lamellipodium, the middle segment containing the nucleus, and the uropodium (Fig. 1). Each segment contained at least three defined regions of interest placed over the cytosol, excluding the nucleus region. The measured values for the three regions were combined in one single value representing one segment. Only adherent and polarized cells were measured. Since B16V cells adhere but do not polarize on collagen type I, the experiments with those cells were performed on a basement membrane-like matrix on which they do polarize.

NHE1 activity was assessed by using the NH_4^+-prepulse technique (33). Exposing cells to 20 mmol/l NH_4^+ for 100 s leads to an alkalinization of the cytosol. Upon removal of NH_4^+ and Na^+ (isosmotically substituted by $NMDG^+$) pH_i decreases rapidly. pH_i recovers when Na^+ is added again to the superfusate. The initial slope of the change in pH_i after readdition of Na^+ was taken as a measure of NHE1 activity, because these experiments were carried out in absence of HCO_3^-, precluding contributions from Na^+-HCO_3^- cotransporters (29, 40).

Statistical Analysis

All experiments were repeated at least eight times except for the migration experiments mentioned above ($N = 4$). Data are presented as means ± SE and were tested for significance employing Wilcoxon signed-rank test for paired samples, Mann-Whitney *U*-test for independent samples, and Friedman test when more than two groups were compared with each other. If normal distribution could be verified, Student's unpaired *t*-test was applied. The level of significance was set at $p < 0.05$ unless otherwise stated.

RESULTS

Immunolocalization of NHE1

As shown for various other cell lines including MV3, MDCK-F, and endothelial cells (3, 11, 16, 37), NHE1 also accumulated at the leading edge of migrating murine melanoma cells and NIH3T3 fibroblasts (Fig. 2).

Intracellular pH

Local pH measurements revealed significant differences in pH_i between the front and the rear end (ΔpH_i front-rear) in all

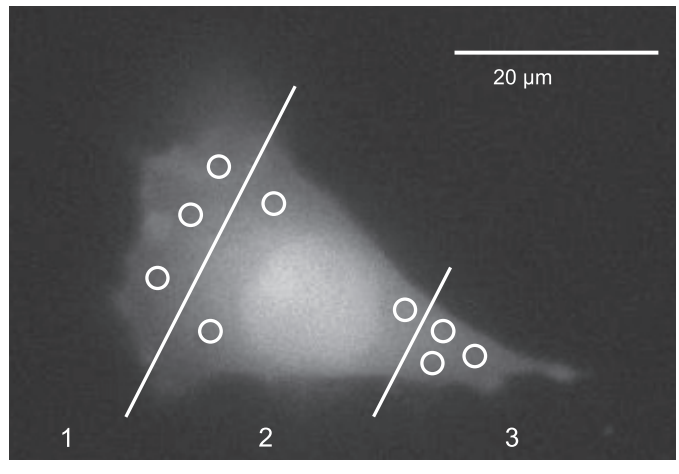

Fig. 1. Measurement of intracellular pH (pH_i) gradients. A sample cell (MV3) is loaded with the proton-sensitive fluorescein-conjugate BCECF. For analysis, the images are divided into three segments (*1-3*; front, middle, rear). Each segment contains at least three defined regions of interest placed over the cytosol while explicitly excluding the nucleus region. A mean value of the three regions of interest is calculated for each segment. See text for further details.

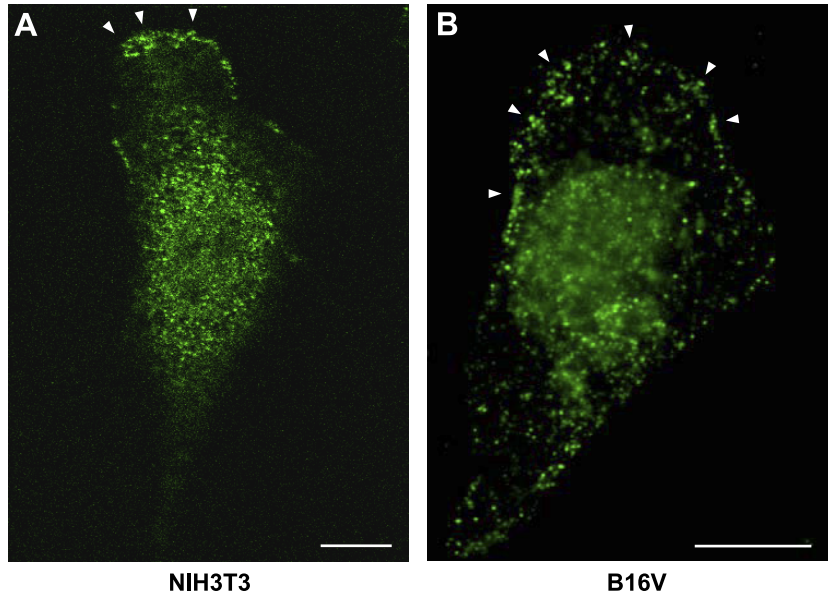

Fig. 2. Immunolocalization of Na^+/H^+ exchanger NHE1 in murine fibroblasts (NIH3T3) and melanoma cells (B16V). NHE1 accumulation at the leading edge (arrowheads) of both migrating fibroblasts (*A*) and migrating murine melanoma cells (*B*) is clearly seen. The two cell lines were prepared slightly differently and labeled with two different antibodies as described in MATERIAL AND METHODS. Scale bars, 10 μm.

investigated cell lines (Fig. 3). Measured in HEPES-buffered Ringer solution, the mean ΔpH_i front-rear averaged 0.16 ± 0.02 pH units in MV3, 0.15 ± 0.05 pH units in B16V, 0.05 ± 0.02 pH units in both NIH3T3 and MDCK-F, and 0.07 ± 0.02 pH units in EA.hy926 cells. Except in the NIH3T3 cells, the pH_i value of the middle segment was always found between the

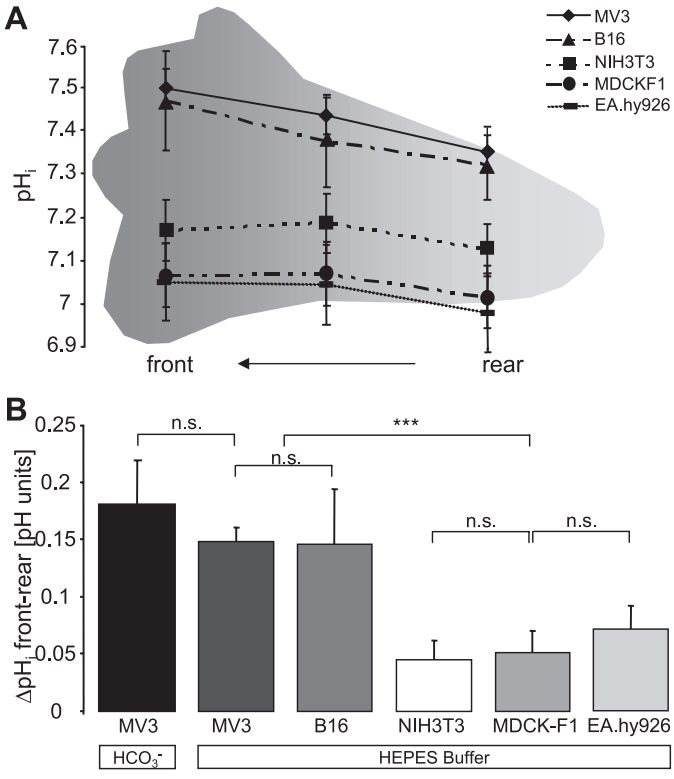

Fig. 3. pH_i gradients in migrating cells. Local pH_i was measured ratiometrically using BCECF. *A*: pH_i gradients along the axis of movement are present in all investigated cell lines (*n* varies between 8 and 32 cells depending on the cell line). *B*: the pH_i difference between the cell front and its rear end (ΔpH_i front-rear) is significant in the two melanoma cell lines (B16V, MV3); ***$P \leq 0.001$. NS, not significant.

pH_i values of the front and rear segment, indicating that the measured differences in cytosolic pH mirror a pH_i gradient along the longitudinal axis of the cell body. To exclude that the gradient is caused or enhanced by the absence of HCO_3^- in the experimental solution, pH_i of MV3 cells was measured also in HCO_3^--buffered Ringer solution. Under these conditions, ΔpH_i front-rear averaged 0.18 ± 0.04 pH units, underlining the physiological significance of the gradient.

NHE1 Dependence of the pH_i Gradient in MV3 and B16V Cells

Because pH_i gradients were most distinct in the two melanoma cell lines, these cells were used to investigate whether NHE1 activity contributes to the generation of the pH_i gradients. Upon inhibition of NHE1 by applying either the specific NHE1 inhibitor HOE642 or a Na^+-free Ringer solution, the cells acidified. Acidification of the cytosol was most prominent at the leading edge corresponding to the localization of NHE1 at the cell front. In MV3 cells the ΔpH_i front-rear decreased from 0.16 ± 0.02 pH units to 0.08 ± 0.03 pH units when exposed to HOE642 and to 0.09 ± 0.02 pH units when exposed to a Na^+-free solution. In B16V cells exposed to HOE642, no differences in pH_i between the front and the rear end were detectable (Fig. 4). Thus, inhibition of NHE1 caused the pH_i gradient to flatten or disappear, accompanied by a general decline in pH_i, demonstrating that the establishment of pH_i gradients to a great extent depends on NHE1 activity.

Subcellular Distribution of NHE1 Activity in MV3 and NIH3T3 Cells

Since pH_i gradients depended on NHE1, an NHE1 activity gradient seemed supposable. Applying the NH_4^+-prepulse technique and using the same arrangement of regions as for the pH_i measurements, NHE1 activity was quantified along the longitudinal axis of the cell. Corresponding to the NHE1 accumulation at the leading edge, its activity was found to be the highest at the cell front (Fig. 5*B*). After an acid load, MV3 cells recovered at a rate of 0.37 ± 0.07 pH units/min at their

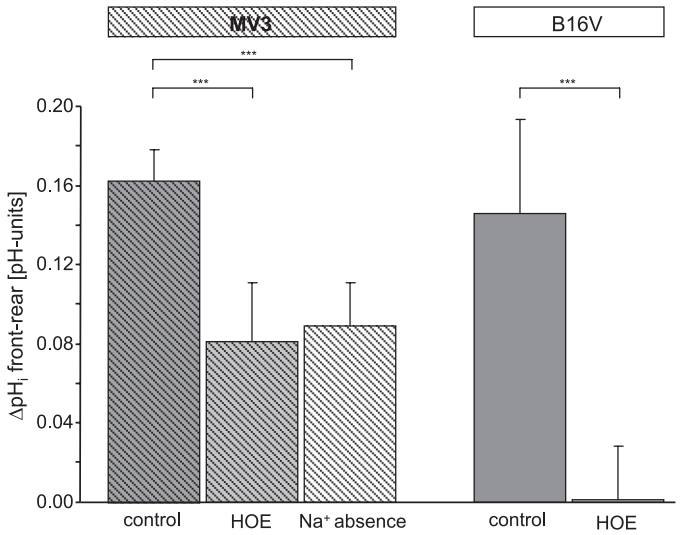

Fig. 4. Contribution of NHE1 activity to the pH_i gradient, given as change in ΔpH_i front-rear. In MV3 cells (hatched bars), inhibition of NHE1 with 10 μM HOE642 ($n = 15$) or by removal of Na^+ ($n = 17$) causes the pH_i gradient to flatten within 5 min. In B16V cells the pH_i gradient vanishes completely within 5 min upon addition of HOE642 ($n = 9$). ***$P \leq 0.001$.

front, 0.32 ± 0.06 pH units/min in the middle segment, and 0.3 ± 0.06 pH units/min at their rear. NIH3T3 cells recovered at a rate of 0.3 ± 0.06 pH units/min at their front, 0.29 ± 0.06 pH units/min in the middle segment, and 0.26 ± 0.06 pH units/min at their trailing end. In addition to immunofluorescence analysis of NHE1 distribution, both the NHE1 inhibition experiments and the subcellular activity measurements provide physiological evidence for the uneven NHE1 distribution in migrating cells and its contribution to the establishment of an intracellular pH gradient.

DISCUSSION

The hypothesis that NHE1 activity may generate small but still important pH gradients either extra- or intracellularly has been around for some time (11, 34). The presence of an extracellular pH gradient at the cell surface and its functional importance in facilitating cell migration has already been shown for human melanoma cells (37, 40). Cells that do not express a functional NHE1 or whose NHE1 is inhibited do not establish a pH gradient at the cell surface nor do they migrate. In human melanoma cells that exhibit normal NHE1 activity, partial removal of the glycocalyx causes the extracellular pH gradient to collapse and the migratory activity to decrease considerably (18). In these cells, however, the cell surface pH-gradient as well as the migratory activity can be restored by stimulating NHE1 activity (18). Here, we demonstrate a complementary, NHE1-dependent, intracellular pH gradient not only present in melanoma but also in other migrating cells. Upon inhibition of NHE1, both the pH_i-gradient (this study) and the cell surface pH-gradient (37) flatten and melanoma cell migration is hindered (36). Changes in the overall extracellular pH cannot compensate for the loss of the cell surface pH-gradient (40). Correspondingly, Tominaga and Barber (41) found that, in the absence of NHE1 activity, cell adhesion and spreading were impaired and pH_i decreased. An overall alkalinization of the cytosol did not rescue the delay in cell adhesion or spreading (41). These results demonstrate the importance of local pH regulation in facilitating cell migration. Since both the extracellular pH-sensitive cell surface/matrix interaction (18, 19) and many components of the intracellular migratory machinery are regulated in a pH-dependent manner, the existence of both pH gradients seems to be most advantageous for migrating cells.

After adhering to the surrounding matrix, migrating cells polarize, defining the direction of movement. As a major regulator of this polarization, the small GTPase Cdc42 accumulates at the cell front (27), where it induces actin polymerization via the Wiskott-Aldrich syndrome protein (WASP) and the Arp 2/3 complex (12, 25) as well as through the Rac/Cdc42 effector IQ-motif-containing GTPase-activating protein 1 (IQGAP1) (2). As shown for migrating fibroblasts, activation of Cdc42 requires H^+ efflux by NHE1 (10), which implies a fundamental role of pH_i in positive feedback loops at the leading edge necessary for enduring cell polarization and directed movement.

Furthermore, the polymerization and depolymerization of actin filaments are coordinated pH-dependently. The generation of free barbed filament ends by the activity of the actin-severing protein cofilin promotes dynamic actin polymerization (45) and membrane protrusion at the cell front. The ability

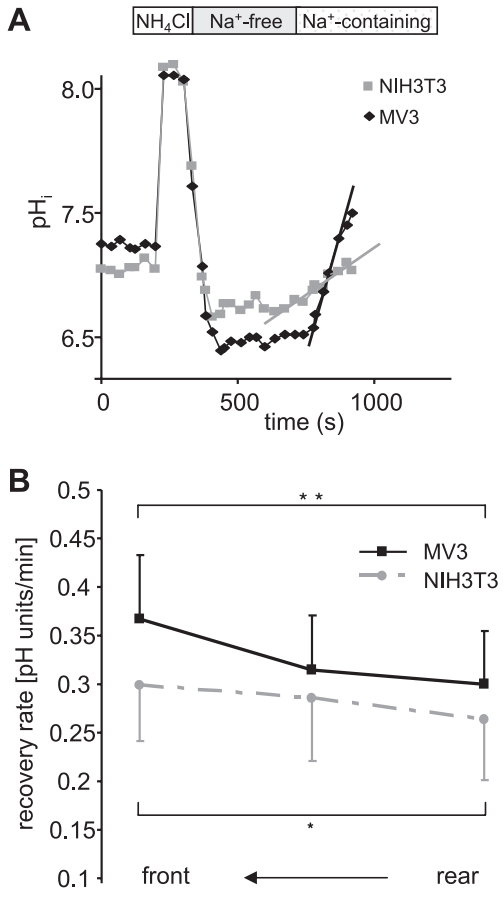

Fig. 5. NHE1 activity in MV3 and NIH3T3 cells. *A*: representative measurements obtained employing the NH_4^+-prepulse technique. After readdition of Na^+ to the HEPES-buffered solution, both MV3 and NIH3T3 cells recover their steady-state pH_i, indicating NHE1 activity. *B*: NHE1 activity at specific regions of the cell. Both cell lines recover at a higher rate at their leading edge than at their rear end [$n = 8$ for MV3 (**$P \leq 0.01$) and $n = 10$ for NIH3T3 (*$P \leq 0.05$) cells].

of cofilin to sever F-actin is stronger at more alkaline pH values (46) due to an increased inhibition of cofilin by pH-dependent phosphoinositide binding at more acidic pH (9). Another actin-binding protein regulating actin assembly and disassembly, gelsolin, is activated by more acidic pH values (1) as can be found at the rear end of migrating melanoma cells. It is tempting to assume that gelsolin is involved in actin recycling at the rear end of migrating cells whereas cofilin regulates actin dynamics at the leading edge. Those are only two of several examples of how migratory events depend on an optimal pH environment (13, 35, 38).

Thus, the pH_i gradient appears to be a prerequisite for cell migration, and the question arises as to whether its slope might function as a "cruise control system." As a matter of fact, H-ras-transfected NIH3T3 migrate faster than wild-type NIH3T3 (28), show an increased net acid extrusion (15), and tend to establish a steeper pH_i gradient [ΔpH_i front-rear: 0.07 ± 0.01 for NIH3T3-ras ($n = 9$) vs. 0.05 ± 0.02 for wild-type NIH3T3 ($n = 10$; $P = 0.14$)]. On the other hand, a comparison of the five investigated cell lines regarding migratory speed is hardly feasible due to their different origins including their different demands on their substrate/matrix components.

In conclusion, we demonstrate here that unevenly distributed NHE1 activity establishes a pH_i gradient along the axis of movement in migrating cells of multiple different origins. We hypothesize that the establishment of this pH_i gradient represents one mechanism by which NHE1 activity promotes cell migration.

ACKNOWLEDGMENTS

Mark Musch, University of Chicago, is gratefully acknowledged for the kind gift of NHE1 antibody, and Jürgen Pünter at Sanofi Aventis for the kind gift of Cariporide.

GRANTS

This work was supported by the Deutsche Forschungsgemeinschaft (STO-654/3-2), the Rolf-Dierichs-Stiftung, a scholarship to C. Martin awarded by the fund "Innovative Medical Research" of the University of Münster Medical School (MA 6 2 08 06), and by the Danish Council for Independent Research (SFP).

DISCLOSURES

No conflicts of interest, financial or otherwise, are declared by the author(s).

REFERENCES

1. **Azuma T, Witke W, Stossel TP, Hartwig JH, Kwiatkowski DJ.** Gelsolin is a downstream effector of rac for fibroblast motility. *EMBO J* 17: 1362–1370, 1998.
2. **Charest PG, Firtel RA.** Big roles for small GTPases in the control of directed cell movement. *Biochem J* 401: 377–390, 2007.
3. **Cutaia MV, Parks N, Centracchio J, Rounds S, Yip KP, Sun AM.** Effect of hypoxic exposure on Na^+/H^+ antiport activity, isoform expression, and localization in endothelial cells. *Am J Physiol Lung Cell Mol Physiol* 275: L442–L451, 1998.
4. **Denker SP, Barber DL.** Cell migration requires both ion translocation and cytoskeletal anchoring by the Na-H exchanger NHE1. *J Cell Biol* 159: 1087–1096, 2002.
5. **Dieterich P, Klages R, Preuss R, Schwab A.** Anomalous dynamics of cell migration. *Proc Natl Acad Sci USA* 105: 459–463, 2008.
6. **Dordick RS, Brierley GP, Garlid KD.** On the mechanism of A23187-induced potassium efflux in rat liver mitochondria. *J Biol Chem* 255: 10299–10305, 1980.
7. **Edgell CJ, McDonald CC, Graham JB.** Permanent cell line expressing human factor VIII-related antigen established by hybridization. *Proc Natl Acad Sci USA* 80: 3734–3737, 1983.
8. **Formelli F, Rossi C, Supino R, Parmiani G.** In vivo characterization of a doxorubicin resistant B16 melanoma cell line. *Br J Cancer* 54: 223–233, 1986.
9. **Frantz C, Barreiro G, Dominguez L, Chen X, Eddy R, Condeelis J, Kelly MJ, Jacobson MP, Barber DL.** Cofilin is a pH sensor for actin free barbed end formation: role of phosphoinositide binding. *J Cell Biol* 183: 865–879, 2008.
10. **Frantz C, Karydis A, Nalbant P, Hahn KM, Barber DL.** Positive feedback between Cdc42 activity and H^+ efflux by the Na-H exchanger NHE1 for polarity of migrating cells. *J Cell Biol* 179: 403–410, 2007.
11. **Grinstein S, Woodside M, Waddell TK, Downey GP, Orlowski J, Pouyssegur J, Wong DC, Foskett JK.** Focal localization of the NHE-1 isoform of the Na^+/H^+ antiport: assessment of effects on intracellular pH. *EMBO J* 12: 5209–5218, 1993.
12. **Heasman SJ, Ridley AJ.** Mammalian Rho GTPases: new insights into their functions from in vivo studies. *Nat Rev Mol Cell Biol* 9: 690–701, 2008.
13. **Hoffmann EK, Lambert IH, Pedersen SF.** Physiology of cell volume regulation in vertebrates. *Physiol Rev* 89: 193–277, 2009.
14. **Jainchill JL, Aaronson SA, Todaro GJ.** Murine sarcoma and leukemia viruses: assay using clonal lines of contact-inhibited mouse cells. *J Virol* 4: 549–553, 1969.
15. **Kaplan DL, Boron WF.** Long-term expression of c-H-ras stimulates Na-H and Na(+)-dependent Cl-HCO_3 exchange in NIH-3T3 fibroblasts. *J Biol Chem* 269: 4116–4124, 1994.
16. **Klein M, Seeger P, Schuricht B, Alper SL, Schwab A.** Polarization of Na(+)/H(+) and Cl(−)/HCO (3)(−) exchangers in migrating renal epithelial cells. *J Gen Physiol* 115: 599–608, 2000.
17. **Koivusalo M, Welch C, Hayashi H, Scott CC, Kim M, Alexander T, Touret N, Hahn KM, Grinstein S.** Amiloride inhibits macropinocytosis by lowering submembranous pH and preventing Rac1 and Cdc42 signaling. *J Cell Biol* 188: 547–563.
18. **Krahling H, Mally S, Eble JA, Noel J, Schwab A, Stock C.** The glycocalyx maintains a cell surface pH nanoenvironment crucial for integrin-mediated migration of human melanoma cells. *Pflügers Arch* 458: 1069–1083, 2009.
19. **Lehenkari PP, Horton MA.** Single integrin molecule adhesion forces in intact cells measured by atomic force microscopy. *Biochem Biophys Res Commun* 259: 645–650, 1999.
20. **Naffar-Abu-Amara S, Shay T, Galun M, Cohen N, Isakoff SJ, Kam Z, Geiger B.** Identification of novel pro-migratory, cancer-associated genes using quantitative, microscopy-based screening. *PLoS One* 3: e1457, 2008.
21. **Oberleithner H, Westphale HJ, Gassner B.** Alkaline stress transforms Madin-Darby canine kidney cells. *Pflügers Arch* 419: 418–420, 1991.
22. **Plopper GE, McNamee HP, Dike LE, Bojanowski K, Ingber DE.** Convergence of integrin and growth factor receptor signaling pathways within the focal adhesion complex. *Mol Biol Cell* 6: 1349–1365, 1995.
23. **Puklin-Faucher E, Sheetz MP.** The mechanical integrin cycle. *J Cell Sci* 122: 179–186, 2009.
24. **Putney LK, Denker SP, Barber DL.** The changing face of the Na^+/H^+ exchanger, NHE1: structure, regulation, and cellular actions. *Annu Rev Pharmacol Toxicol* 42: 527–552, 2002.
25. **Raftopoulou M, Hall A.** Cell migration: Rho GTPases lead the way. *Dev Biol* 265: 23–32, 2004.
26. **Rasmussen M, Alexander RT, Darborg BV, Mobjerg N, Hoffmann EK, Kapus A, Pedersen SF.** Osmotic cell shrinkage activates ezrin/radixin/moesin (ERM) proteins: activation mechanisms and physiological implications. *Am J Physiol Cell Physiol* 294: C197–C212, 2008.
27. **Ridley AJ, Schwartz MA, Burridge K, Firtel RA, Ginsberg MH, Borisy G, Parsons JT, Horwitz AR.** Cell migration: integrating signals from front to back. *Science* 302: 1704–1709, 2003.
28. **Schneider L, Klausen TK, Stock C, Mally S, Christensen ST, Pedersen SF, Hoffmann EK, Schwab A.** H-ras transformation sensitizes volume-activated anion channels and increases migratory activity of NIH3T3 fibroblasts. *Pflügers Arch* 455: 1055–1062, 2008.
29. **Schneider L, Stock CM, Dieterich P, Jensen BH, Pedersen LB, Satir P, Schwab A, Christensen ST, Pedersen SF.** The Na^+/H^+ exchanger NHE1 is required for directional migration stimulated via PDGFR-alpha in the primary cilium. *J Cell Biol* 185: 163–176, 2009.
30. **Schwab A.** Function and spatial distribution of ion channels and transporters in cell migration. *Am J Physiol Renal Physiol* 280: F739–F747, 2001.

31. **Schwab A, Finsterwalder F, Kersting U, Danker T, Oberleithner H.** Intracellular Ca^{2+} distribution in migrating transformed epithelial cells. *Pflügers Arch* 434: 70–76, 1997.
32. **Schwab A, Reinhardt J, Schneider SW, Gassner B, Schuricht B.** K(+) channel-dependent migration of fibroblasts and human melanoma cells. *Cell Physiol Biochem* 9: 126–132, 1999.
33. **Schwab A, Rossmann H, Klein M, Dieterich P, Gassner B, Neff C, Stock C, Seidler U.** Functional role of Na^+-HCO_3^- cotransport in migration of transformed renal epithelial cells. *J Physiol* 568: 445–458, 2005.
34. **Srivastava J, Barber DL, Jacobson MP.** Intracellular pH sensors: design principles and functional significance. *Physiology (Bethesda)* 22: 30–39, 2007.
35. **Srivastava J, Barreiro G, Groscurth S, Gingras AR, Goult BT, Critchley DR, Kelly MJ, Jacobson MP, Barber DL.** Structural model and functional significance of pH-dependent talin-actin binding for focal adhesion remodeling. *Proc Natl Acad Sci USA* 105: 14436–14441, 2008.
36. **Stock C, Gassner B, Hauck CR, Arnold H, Mally S, Eble JA, Dieterich P, Schwab A.** Migration of human melanoma cells depends on extracellular pH and Na^+/H^+ exchange. *J Physiol* 567: 225–238, 2005.
37. **Stock C, Mueller M, Kraehling H, Mally S, Noel J, Eder C, Schwab A.** pH nanoenvironment at the surface of single melanoma cells. *Cell Physiol Biochem* 20: 679–686, 2007.
38. **Stock C, Schwab A.** Protons make tumor cells move like clockwork. *Pflügers Arch* 458: 981–992, 2009.
39. **Stock C, Schwab A.** Role of the Na/H exchanger NHE1 in cell migration. *Acta Physiol (Oxf)* 187: 149–157, 2006.
40. **Stuwe L, Muller M, Fabian A, Waning J, Mally S, Noel J, Schwab A, Stock C.** pH dependence of melanoma cell migration: protons extruded by NHE1 dominate protons of the bulk solution. *J Physiol* 585: 351–360, 2007.
41. **Tominaga T, Barber DL.** Na-H exchange acts downstream of RhoA to regulate integrin-induced cell adhesion and spreading. *Mol Biol Cell* 9: 2287–2303, 1998.
42. **Vahle AK, Fabian A, Mally S, Schwab A, Stock C.** Na^+/H^+ exchange promotes adhesion, motility, and invasiveness of mouse melanoma cells (Abstract). *Acta Physiol* 189: 149, 2007.
43. **Van Muijen GN, Jansen KF, Cornelissen IM, Smeets DF, Beck JL, Ruiter DJ.** Establishment and characterization of a human melanoma cell line (MV3) which is highly metastatic in nude mice. *Int J Cancer* 48: 85–91, 1991.
44. **Vincourt JB, Etienne S, Cottet J, Delaunay C, Malanda B, Lionneton F, Sirveaux F, Netter P, Plenat F, Mainard D, Vignaud JM, Magdalou J.** C-propeptides of procollagens Ialpha1 and II that differentially accumulate in enchondromas versus chondrosarcomas regulate tumor cell survival and migration. *Cancer Res* 70: 4739–4748.
45. **Wang W, Eddy R, Condeelis J.** The cofilin pathway in breast cancer invasion and metastasis. *Nat Rev Cancer* 7: 429–440, 2007.
46. **Yonezawa N, Nishida E, Sakai H.** pH control of actin polymerization by cofilin. *J Biol Chem* 260: 14410–14412, 1985.